Eur J Nucl Med (1988) 14:403–407

European Journal of Nuclear Medicine

The appended curve technique for deconvolutional analysis – method and validation

Jack E. Juni[1], James H. Thrall[2], Jerry W. Froelich[2], Roger C. Wiggins[3], Darrell A. Campbell, Jr[3], and Michael Tuscan[3]

[1] William Beaumont Hospital, Department of Nuclear Medicine, 44201 Dequindre Road, Troy, MI 48098-1198, USA
[2] Henry Ford Hospital, Detroit, Michigan, USA
[3] University of Michigan Medical Center, Departments of Internal Medicine and Surgery, Ann Arbor, Michigan, USA

Abstract. Deconvolutional analysis (DCA) is useful in correction of organ time activity curves (response function) for variations in blood activity (input function). Despite enthusiastic reports of applications of DCA in renal and cardiac scintigraphy, routine use has awaited an easily implemented algorithm which is insensitive to statistical noise. The matrix method suffers from the propagation of errors in early data points through the entire curve. Curve fitting or constraint methods require prior knowledge of the expected form of the results. DCA by Fourier transforms (FT) is less influenced by single data points but often suffers from high frequency artifacts which result from the abrupt termination of data acquisition at a nonzero value.

To reduce this artifact, we extend the input (i) and response curves to three to five times the initial period of data acquisition (P) by appending a smooth low frequency curve with a gradual taper to zero. Satisfactory results have been obtained using a half cosine curve of length 2–3P. The FTs of the input and response I and R, are computed and R/I determined. The inverse FT is performed and the curve segment corresponding to the initial period of acquisition (P) is retained. We have validated this technique in a dog model by comparing the mean renal transit times of ^{131}I-iodohippuran by direct renal artery injection to that calculated by deconvolution of an intravenous injection. The correlation was excellent ($r=0.97$, $P<0.005$).

The extension of the data curves by appending a low frequency "tail" before DCA reduces the data termination artifact. This method is rapid, simple, and easily implemented on a microcomputer. Excellent results have been obtained with clinical data.

Key words: Deconvolution – Pharmacokinetics – Transit time – Filters – Algorithm

Quantitative measurements of tracer kinetics are an important part of nuclear medicine. The dynamic pattern of tracer activity over a given organ may be influenced by many factors other than the function of that organ. Quality of bolus injection, systemic recirculation of tracer, and multicompartmental removal of blood pool activity all may potentially alter or distort the temporal pattern of activity seen at the organ of interest. These complicating factors hamper, and may defeat, attempts to accurately assess isolated organ function.

Deconvolutional analysis is a mathematical technique which can correct an organ's time activity curve for the dynamically changing pattern of blood pool activity being presented to that organ. Several techniques of deconvolution have been described in the medical literature (Valentinuzzi and Montaldo 1975; Williams 1979; Kenney et al. 1975; Alderson et al. 1979; Gamel et al. 1973; Nakamura et al. 1982; Kuruc et al. 1983) each with disadvantages which have hindered routine clinical use.

We have developed and validated a method of deconvolutional analysis which provides excellent results with clinical scintigraphic data. We have also investigated the correlation of organ impulse response functions (IRF) obtained in-vivo by deconvolution following intravenous and direct intra-arterial injection of tracer.

Methods

Deconvolution of scintigraphic data by the division of Fourier transforms has been reported by several groups (Alderson et al. 1979; Gamel et al. 1973; Kuruc et al. 1983). Unfortunately, the abrupt termination of data collection while organ radioactivity remains at a nonzero value results in an sharp discontinuity in the data curves. This discontinuity results in high frequency artifacts in the computed IRF. In order to reduce this artifact, we have developed a modification of the Fourier transform technique. This technique is illustrated graphically in Figs. 1 and 2. Figure 1a shows an example pair of time activity curves derived from a ^{99m}Tc-disofenin hepatobiliary study. Data was collected at 1 min intervals for 32 min. The blood pool or input function curve was derived from a region of interest over the heart. The liver time activity curve is used as the response function. Figure 1b shows the original data curves from Fig. 1a on an *expanded* time scale of 0–256 min. The abrupt discontinuity at the end of data collection is clearly seen.

A smoothly tapering, low frequency curve is appended to each of the original data curves in such a manner as to make the curves gradually and smoothly taper to zero (Fig. 2a). This lengthens the original curve several fold. The shape of the appended curve or tail is not particularly critical and is choosen to consist primarly of very low frequencies relative to the original data and to provide a smooth transition with the terminal points of the original data. We have found that a raised one-half cosine wave with an initial

Offprints requests to: J.E. Juni

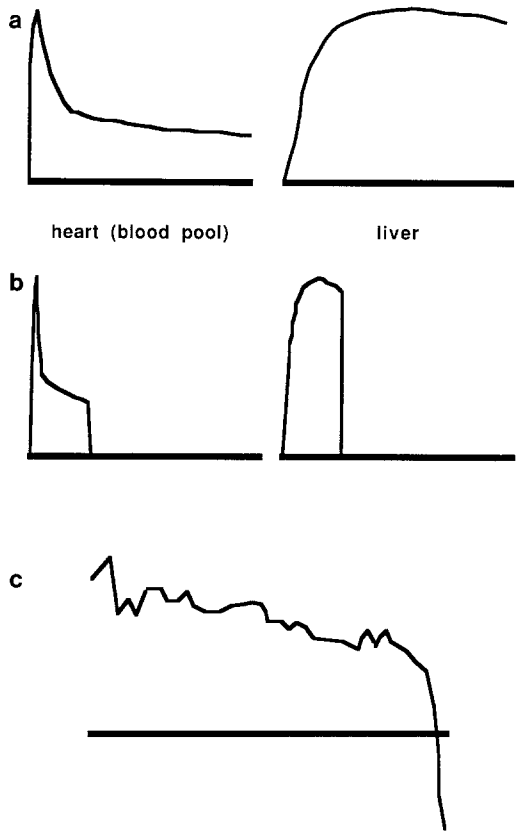

Fig. 1. a Time activity curves derived from the heart and liver following intravenous injection of ^{99m}Tc-disofenin (DISIDA). Data was collected at 1 min intervals for 32 min. **b** Same data as shown in Fig. 1a but on an *expanded* time scale of 0–256 min. The abrupt continuity caused by termination of data acquisition is evident. **c** Result of deconvolution of the curves in Fig. 1a by direct division of Fourier transforms. Note the large artifact caused by the abrupt termination of data collection

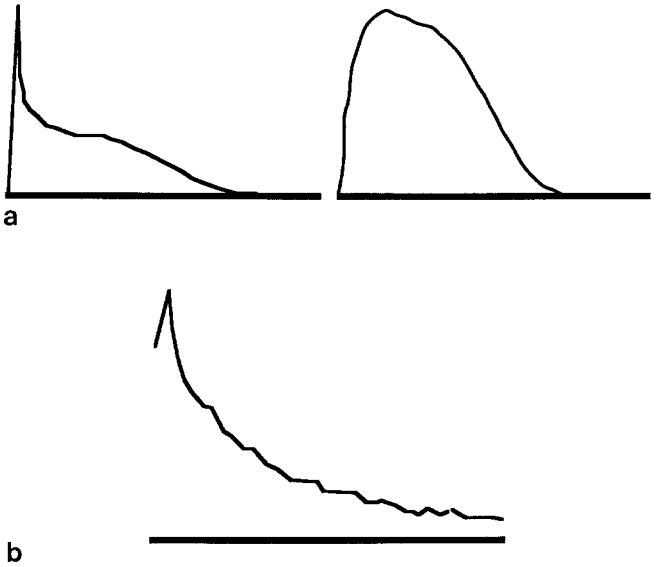

Fig. 2. a The original data curves from Fig. 1 are extended by appending a smoothly tapering, low frequency curve. *Time scale 0–256 min.* **b** Results of deconvolution by the appended curve method. *Time scale 0–32 min*

amplitude equal to that of the terminal points of the original data series gives good results. In general, as the tail is made longer, the high frequency artifact in the resulting computed IRF is further reduced. As a minimum, an appended curve of at least three times the original data series is usually required.

The Fourier transforms of the resulting extended curves are calculated by a standard fast Fourier transform (FFT) algorithm (Cooley and Tukey 1965). The resulting frequency domain organ curve is divided by the frequency domain blood pool curve. An inverse Fourier transform is performed yielding a time domain curve several times longer than the original data curves. The initial portion of this curve, representing the actual period of data collection, is the computed impulse response function. The remainder of the curve is ignored. Figure 2b shows the resulting impulse response function displayed on the original time scale of 0–32 min.

Simulation study. In order to compare this "appended curve" technique to other methods of deconvolution described in the medical literature, a simulation study was performed. A gamma variate function was generated to simulate an ideal organ impulse response function. An idealized blood pool curve was generated from a different gamma variate function with added re-circulation. The organ response was then simulated by convolving the blood pool and organ impulse response curves.

Random noise was added to both the simulated blood pool and simulated organ curve in a Poisson distribution to simulate the statistical noise encountered in a typical scintigraphic study. The amount of noise added was calculated assuming an average count rate of 1000–2000 counts per point with a peak of 6000 counts. The impulse response function (IRF) was calculated from this noisy data by the appended curve technique as well as by two techniques previously employed in the medical literature, discrete deconvolution by the matrix inversion method of Valentinuzzi and Montaldo (1975) and direct division of Fourier transforms as used by Alderson et al. (1979), with and without use of a lowpass smoothing filter. The IRF calculated by each of these techniques was compared to the original noise free simulated impulse response function and the root mean squared error was calculated. This process was repeated 50 times for each technique.

Since most clinical trials of deconvolution have used extensive data smoothing, the discrete matrix inversion method and the appended curve method were also evaluated after first smoothing each noise added curve three times with a standard three point weighted (1–2–1) smoothing algorithm. The average error in calculation of the IRF by each technique is shown in Table 1.

In-vivo validation. The IRF obtained by deconvolution after intravenous injection of tracer would be expected to mirror

Table 1. Computer simulation of noisy data root mean squared error ±1 S.D.

	Matrix method	Fourier transform	Fourier transform + Tail
Unsmoothed	$>10^{33}$	9.10±13.9	0.87±1.12
Smoothed	2.9±20.6	2.1 ± 5.3	0.35±0.28

the pattern seen with direct arterial injection into an organ. The appended curve technique was validated by examining this correlation in a dog kidney model.

As part of an unrelated study, each dog had one kidney removed. An indwelling catheter was placed directly in the renal artery of the remaining kidney, under conditions where patency of the catheter was maintained by constant infusion of 0.15 µl/hour NaCl from a freon driven implanted pump. Animals were studied several days after surgery as previously described (Campbell et al. 1983). When renal functions were stable each dog was anethetised with intravenous sodium pentobarbital. Each animal received a rapid bolus intra-arterial injection of 0.125 mCi (4.63 mBq) ^{131}I-ortho-iodohippurate. Sequential gamma camera images of the kidney were obtained on a minicomputer at 15 s intervals beginning 1–2 min prior to injection and continuing for 30 min. A renal region of interest was defined and the renal time activity curve generated. This curve represents a direct physical measurement of the renal IRF.

Thirty mins after completion of the intra-arterial study, the animal was reinjected *intravenously* with 0.25 mCi (9.25 mBq) ^{131}I-ortho-iodohippurate. One region of interest was defined over the heart and another over the kidney. Time activity curves were then generated for the blood pool and kidney. After several applications of a three point weighted smooth to the renal time activity curve, deconvolution was performed by the appended curve technique to calculate the renal impulse response function. A total of five combined intra-arterial and intravenous studies were performed. The mean transit time of tracer through the kidney was calculated for both the directly measured and the calculated renal impulse response function by dividing the area under the IRF curve by the height of the curve.

Results

The simulation data (Table 1) shows a marked reduction in error of the calculated impulse response function when the appended curve technique is used. Without prior data smoothing, the matrix inversion technique became so unstable as to make quantification of error meaningless. Deconvolution by the direct division of Fourier transforms without appended curves showed significantly greater error than that obtained by the appended curve technique ($P<0.01$). Even after data smoothing, the appended curve technique provided significantly better recovery of the impulse response function than the matrix inversion technique or the direct Fourier transforms method.

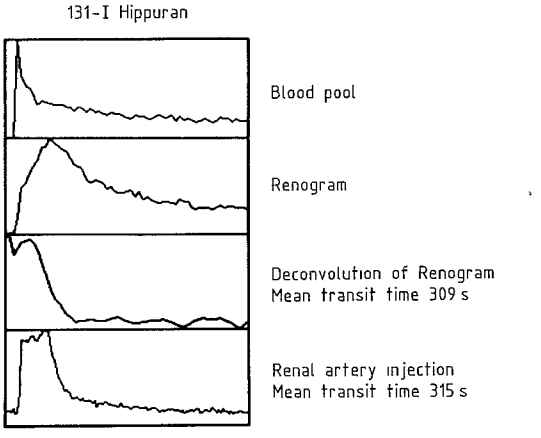

Fig. 3. Time activity curves obtained in a normal dog following direct injection in the renal artery (below), and in the same dog following intravenous injection of ^{131}I-hippuran. Heart (blood pool) and renal curves from the intravenous injection are shown above. The renal impulse response function calculated by deconvolution is shown second from the bottom. Note the simularity in both appearance and calculated mean transit times of the calculated response function and that following direct measured injection into the renal artery. Time scale 0–32 min

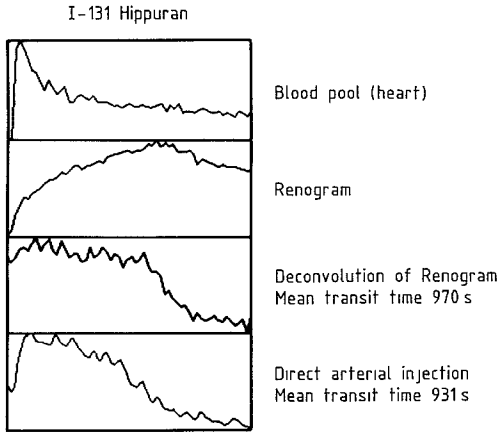

Fig. 4. Measured and calculated time activity curves obtained from a dog suffering from drug induced renal dysfunction. The order of curves is similar to that in Fig. 3

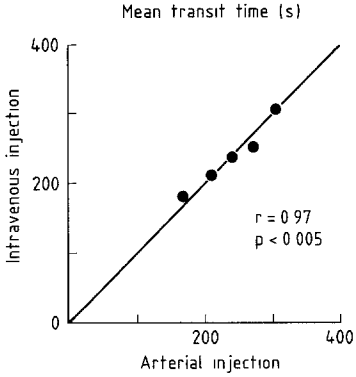

Fig. 5. Correlation of ^{131}I-hippuran mean transit times calculated from direct renal artery injection and from intravenous injection with deconvolution performed by the appended curve technique ($r=0.97$, $P<0.005$)

The in vivo study was done to correlate the renal impulse response function as obtained by direct renal artery injection to that obtained by deconvolution of an intravenous injection. Typical curves obtained in two dogs are shown in Figs. 3 and 4. The overall appearance of the curves is quite similar. The mean transit times calculated from the intravenous injection are compared to those obtained by intra-arterial injection (Fig. 5). An excellent correlation between the calculated and the measured values is seen ($r=0.97$, $P<0.005$).

Discussion

The goal of deconvolutional analysis in clinical imaging is typically the reconstruction of an organ's IRF from the observed blood pool and organ time activity (or time den-

sity) curves. The IRF represents the calculated pattern of activity that *would have been observed* had tracer been injected as a single infinitely narrow bolus directly into the organ's blood supply with no systemic tracer recirculation. The IRF represents the organ's tracer kinetics in the simplest and most direct possible way, uncontaminated by the blurring effects of recirculation of tracer or the inevitable delay or spreading of a bolus injection. Ideally the IRF reflects the tracer kinetics of only the organ of interest and is not influenced by the effects of other organs or organ systems on the blood pool activity.

All deconvolution techniques tend to magnify noise. Some investigators have devised methods which constrain the results to fit some predetermined model (e.g. a gamma variate or lagged normal density function, or a smooth non-negative continuous function) (Nakamura et al. 1982; Kuruc et al. 1983). These approaches may give excellent results in specific well defined systems, but all assume a prior knowledge of the shape of the system's impulse response function which may not always be available and are thus not considered here. In those situations for which correct *a priori* information is available, the incorporation of this information into any deconvolution algorithm would be expected to improve results.

Deconvolution to determine the IRF is a complex computational process in the time domain but is relatively straightforward in the frequency domain. The Fourier transform of the IRF may theoretically be obtained simply by dividing the transform of the organ time activity curve by the transform of the blood pool time activity curve:

$$H=\frac{R}{B}$$

where H, R, and B represent the Fourier transforms of the impulse response function, observed response function, and input function respectively. The IRF in the time domain is then obtained by performing an inverse Fourier transform.

Although this technique is appealing in its simplicity, it has several drawbacks which have limited its clinical applicability. Foremost among these is the appearance of high frequency noise in the calculated IRF caused by abrupt discontinuities in the original data curves. Such discontinuities typically occur if data acquisition is terminated while a significant amount of activity remains in the organ of interest or the blood pool. This situation occurs in the great majority of clinical scintigraphic procedures as it is usually impractical to continue data acquisition until tracer is totally cleared from both the blood pool and the organ of interest. In signal processing terms, the abrupt discontinuation of data acquisition may be viewed as a windowing operation in which a rectangular window is applied to the natural, continuously varying data. This rectangular window introduces a number of high frequency components which were not present in the original data.

Figure 1a shows a typical set of blood pool (*left*) and organ (*right*) scintigraphic time activity curves, in this case cardiac and hepatic time activity curves obtained by intravenous injection of ^{99m}Tc-disofenin. Note the abrupt transition to zero which occurs upon termination of data acquisition. Figure 1c shows the impulse response function calculated from this data by the division of Fourier transforms. A great deal of high frequency noise is seen and a large negative artifact has appeared. This curve is clearly a poor representation of actual tracer handling by a body organ.

Several groups have successfully implemented the direct matrix inversion approach in certain applications (Ham 1981; Cosgriff 1982). This approach computes the impulse response function matrix H in a successive manner using the recursion formula:

$$H(t)=R(t)-\sum_{T=0}^{t-1}[B(t-T)\,H(T)]/B(0)$$

where B represents the blood pool or input function and R represents the observed organ response function. While this method may work well with noise free data, the earliest data points have a disproportionately large influence on the computed IRF. Small statistical errors in the initial input function points may cause wide oscillations in the impulse response function.

By virtue of the Poisson counting statistics of scintigraphic data, random fluctuations in observed count rates are inevitable. These fluctuations are proportionally greatest when the count rate is low. In scintigraphic studies, the lowest count rates typically occur in the earliest data points as tracer is still being introduced into the system. Deconvolution by the matrix method causes the random errors in these points to propagate through the entire result. Thus, the matrix inversion technique is most sensitive to noise in the portion of the study with the greatest relative statistical error.

Our method of deconvolution assumes, as do most others, that the system under study is linear, that is, that a given increase in injected activity will result in the same relative increase in the observed response function. This situation does not exist with some pharmaceuticals or bioactive substances as involved receptors or transport mechanisms may become saturated at high doses. The overwhelming majority of radiotracers used in clinical nuclear medicine are administered in such low doses as to avoid saturation or other pharmacological effects. Non-linearity of gamma camera response may be seen at high count rates due to dead time losses. This may be avoided by administration of appropriately low tracer doses. Deconvolutional analysis assumes time invariance of the system under observation, i.e., the system's intrinsic handling of tracer does not change with time. Although all biological systems change with time, physiological equilibrium is assumed for the duration of the tracer study.

Although appending a slowly varying curve to the original data may itself induce artifacts, these would be of very low frequency relative to the impulse response function and would thus cause minimal distortion in the resulting curves. The appended curve may be viewed intuitively as a variation of the rectangular windowing function used in the original data acquisition. Thus, although deconvolution is still performed by the division of Fourier transforms, less of the high frequency components created by the windowing effect of the abrupt cessation of data collection are incorporated into the deconvolution process.

Summary

The clinical usefulness of deconvolution has been demonstrated by others in the setting of renal and cardiac disease. Routine use has awaited a practical technique sufficiently

insensitive to noise and artifacts which does not require prior knowledge of the shape of the organ impulse response function. We have presented a simple method of deconvolution by Fourier transforms that is easily implemented and requires minimal prior assumptions about expected results. It is computationally rapid and, unlike matrix inversion methods, is relatively insensitive to errors in single specific data points. Artifacts induced by the abrupt termination of data collection are significantly reduced. The physician contemplating deconvolutional analysis of a given system can choose between many different algorithms. In those situations for which appropriate a priori information is not available, the appended curve technique described here may provide a practical and reliable alternative.

Acknowledgement. The authors would like to thank Mrs. Vi Rhodes for her excellent secretarial support and continuing patience.

References

Alderson PO, Douglass KH, Mendenhall KG, Guadini VA, Watson DC, Links JM, Wagner HN (1979) Deconvolution analysis in radionuclide quantitation of left-to-right cardiac shunts. J Nucl Med 20:502–506

Campbell DA Jr, Wiggins R, Kunkel S, Niederhuber J (1983) Chronic intrarenal delivery of PGE_1 using an implantable drug delivery system. Am Soc Art Int Organs Transactions 23:344–347

Cooley J, Tukey J (1965) An algorithm for the machine calculation of complex Fourier series. Math Comput 1965, 19:297–301

Cosgriff PS, Berry JM (1982) A comparative assessment of deconvolution and diuresis renography in equivocal upper urinary tract obstruction. Nucl Med Commun 3:377–384

Gamel J, Rousseau WF, Katholi CR, Mesel E (1973) Pitfalls in digital computation of the impulse response of vascular beds from indicator-dilution curves. Circ Res 32:516–523

Ham HR, Dobbeleir A, Viart P, Piepsz A, Lenaers A (1981) Radionuclide quantitation to left-to-right cardiac shunts using deconvolution analysis: Concise Communication. J Nucl Med 22:688–692

Kenney RW, Ackery DM, Fleming JS et al. (1975) Deconvolution analysis of the scintillation camera renogram. Br J Radiol 48:481–486

Kuruc A, Treves S, Parker JA (1983) Accuracy of deconvolution algorithms assessed by simulation studies: Concise Communication. J Nucl Med 24:258–263

Nakamura M, Suzuki Y, Nagasawa T, Sugihara M, Takahashi T (1982) Detection and quantitation of left-to-right shunts from radionuclide angiocardiography using the homomorphic deconvolution technique. IEEE BME 23:192–201

Piepsz A, Ham HR, Erbsmann F (1982) A co-operative study on the clinical value of dynamic renal scanning with deconvolution analysis. Br J Radiol 55:419–433

Valentinuzzi ME, Montaldo VEM (1975) Discrete deconvolution. Med Biol Eng Comput 13:123–125

Williams DL (1979) Improvement in quantitative data analysis by numerical deconvolution techniques. J Nucl Med 20:568–570

Received June 14, 1987 / February 17, 1988